ELECTRON PARAMETRIC INSTABILITIES IN SHORT ULTRAINTENSE LINEARLY-POLARIZED LASER PULSES

H.C. Barr, P. Mason and D.M. Parr

Department of Physics, University of Essex, Colchester, England, CO4 3SQ

Abstract

The relativistic mass increase of electrons quivering in sub-picosecond very intense ($I > 10^{18} Wcm^{-2}$) laser pulses modifies electron parametric instabilities such as Raman scattering, is the source of the relativistic modulational and filamentation instabilities and gives rise to new regimes at laser harmonics. A Lorentz-transformed pulse frame description of electron parametric instabilities driven by linearly polarized light valid for arbitrarily high intensities is presented.

1. Introduction

The relativistic mass increase of electrons in current ultraintense laser pulses causes induced transparency of the plasma, saturation of the electron quiver velocity and gives rise to a new set of parametric instability regimes due to strong mode-coupling [1-3]. The latter generate laser harmonics and are Raman-like when coupling between light waves is due to density fluctuations or are of the relativistic modulational and filamentation type when the coupling is due to fluctuations in the electron mass increase [4-5]. Laser light of frequency and wavenumber $(\omega_0, \mathbf{k}_0)$ couples any fluctuation at $(\omega, \mathbf{k})$ to a hierarchy of fluctuations at $(\omega + n\omega_0, \mathbf{k} + n\mathbf{k}_0)$ where n is an integer. When two or more of these fluctuations simultaneously correspond to resonant modes (or quasimodes) of the laser-plasma system, parametric instability is possible. This is irrespective of whether the laser is circularly polarised (and purely harmonic) or linearly polarised (where the anharmonic electron motion is comprised of harmonics $(n\omega_0, n\mathbf{k}_0)$ each of which can also contribute as pump waves). We adopt an approach which is applicable for any density, laser intensity and polarisation, or scattering geometry. Here we show results for the decay of an intense linearly polarised laser pulse in underdense plasma and look at scattering in the plane of polarisation.

2. Method

For short pulses we perform the analysis in the proper frame of the pulse, i.e. Lorentz-transform to the pulse group velocity $\mathbf{u} = \mathbf{k}_0 c^2 / \omega_0$. The laser pulse phase becomes $\eta = -\omega_0 t' / \gamma_u$ where $\gamma_u = (1 - u^2 / c^2)^{-1/2}$ so that the laser, in this frame, appears as a homogeneous dipole oscillation having zero magnetic field. The exact periodic but anharmonic solution [7] is obtained numerically from the non-linear but simple differential equation

$$\ddot{\mathbf{p}}_0 + \omega_{po}^2 (\mathbf{p}_0 / \gamma_0 + m\mathbf{u}) = 0 \qquad (1)$$

where the pump wave electron momentum is $\mathbf{p}_0$, the mass increase $\gamma_0 = (1 + p_0^{\,2} / m^2c^2)^{1/2}$ and we define a relativistic plasma frequency $\omega_{pr}(t) = \omega_{po} / \gamma_0^{1/2}(t)$ where ω_{po} is the pulse frame plasma frequency. These pump parameters are time dependent only and give no $\mathbf{k}$-space coupling in the linearised equations. When Fourier transformed in space, these can be written in the form (quantities normalised to laser parameters)

$$\ddot{\mathbf{b}} + (\omega_{pr}^2(t) + k^2)\mathbf{b} = ik\mathbf{c}_2(t)(k^2\phi + \omega_{pr}^2(t)(\phi - \dot{\psi})) \quad (2)$$

$$\dot{\phi} + \omega_{pr}^2(t)\psi = -ik^{-1}c_1(t)(k^2\phi + \omega_{pr}^2(t)(\phi - \dot{\psi})) \quad (3)$$

$$\dot{\psi} - \phi = -ikc_1(t)\psi + ik^{-1}\mathbf{c}_2(t)\cdot\mathbf{b} \quad (4)$$

where $\mathbf{b}$ is the magnetic field, ϕ the electric potential and $i\mathbf{k}\phi$ the irrotational part of the electron momentum ($\mathbf{p} = \mathbf{a} + i\mathbf{k}\psi$, $\mathbf{a}$ is the vector potential and $\mathbf{b} = i\mathbf{k}\times\mathbf{a}$). The periodic coupling terms are $c_1(t) = \hat{\mathbf{k}}\cdot\mathbf{p}_0(t)/\gamma_0(t)$, $\mathbf{c}_2(t) = \hat{\mathbf{k}}\times\mathbf{p}_0(t)/\gamma_0(t)$. Since the coefficients are periodic, they admit Floquet solutions whose characteristic exponent gives the dispersion characteristics. The standard procedure is to Fourier analyse in time, obtain an infinite set of coupled-mode equations whose solution gives the dispersion relation. This requires an *analytic* form for the zero order solution which is only available in certain limiting cases[6]. Here we evolve the above system of ordinary differential equations in time for given values of $\mathbf{k}$. The growth is then easily obtained from the time signal after a few e-foldings and the frequencies and mode-structure obtained by applying an FFT routine to the solution after deconvolving the growth.

3. Results

Assume a laser pulse propagating in the **x** direction, plane-polarised in the **x-y** plane whose amplitude is $q = eA_0/mc^2 \approx 8.5\times10^{-10}\lambda_L(\mu m)I_L^{1/2}(Wcm^{-2})$. The dispersion relation in the laboratory frame $\omega_0^2 = \omega_{pr}^2 + k_0^2c^2$ becomes $\omega_0' = \omega_{pr}$ in the pulse frame where $\omega_{pr} = \omega_{po}^{lab} / \gamma_a^{1/2}$ and $\gamma_a = (1 + q^2/2)^{1/2}$. We consider here scattering in the plane of polarisation and choose a density of $n_0 = 0.1n_c$ where n_c is the laser critical density.

Figure 1 is a contour plot of the normalised pulse-frame growth rate ν' / ω_{pr} plotted in the laboratory frame (k_x, k_y)-plane for intensities ranging from weakly to strongly relativistic. A clear pattern of peak growth lobes is apparent which represent a combination of phase matching and optimal driving. As a guide, the dashed lines are the circles $(k_x - nk_0)^2 + k_y^2 = n(n - 2\omega_{pr})$ along which phase matching occurs between a resonant plasma wave $\omega = \omega_{pr}$ and a resonant scattered wave $\omega_s = n\omega_0 - \omega_{pr}$ coupled through n-1 intermediate nonresonant oscillations. We index each maximum growth lobe as $n.m$ where n refers to the harmonic number (dashed circle) and m is an integer counting the peak growth points in a clockwise direction along any given circle. This figure exhibits stimulated back, side and forward Raman scattering (SRBS, SRSS, SRBS) , the relativistic modulational and filamentation instabilities (RMI, RFI) and includes mode-coupling to all orders and driving by all harmonics in the laser driver. The narrow peaks n.1 correspond to SRFS emission

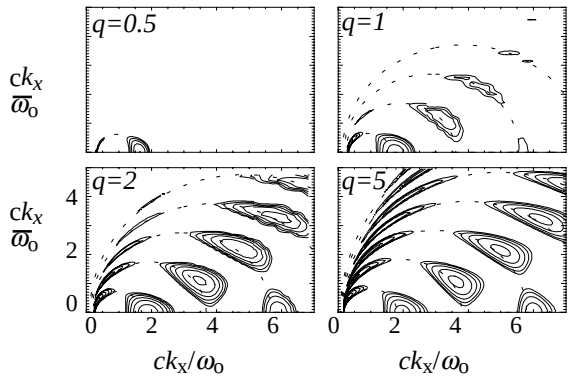

Fig. 1. Contour plot of pulse frame growth rate v'/ω_{pr} versus laboratory (k_x,k_y). Contour range is 0.05(0.02)0.13.

emerging at increasingly oblique angles as n rises. The lobe 1.2 is the usual SRBS. The lobes n.2 for n>1 are SRSS at increasingly oblique directions relative to the backscattering direction. For higher harmonics, new sequences of SRBS and SRSS occur ($m \le (n+3)/2$ for n odd, $m \le (n+2)/2$ for n even). For $q<1$, emission is predominantly at the first harmonic with only weak growth at higher harmonics. Growth at all harmonics rises rapidly with q until $q \approx 1$; thereafter a full complement of lobes appears with comparable growth rates over a wide region of **k**-space representing emission into many harmonics and into a set of well-defined scattering angles. There is only a very slow fall-off in growth with harmonic number [1,2] (this will eventually be limited by Landau damping). Although these lobes lie close to the lines predicted by the phase matching argument above, there is significant deviation from weak coupling theory. The growth is such that $v \sim \omega \sim \omega_{pr}$ and hence is in an intermediate regime between weakly and strongly coupled.

Figure 2 shows a typical multimode structure of modes of $\omega + n\omega_0$ for the lobe 4.1 which corresponds to scattering into the fourth harmonic at an angle of 51° to the forwards direction. The dominant peak at $w = -4w_0 + w_{pr}$ in the vector potential $a(\omega)$ and the peak at $\omega \approx \omega_{pr}$ in the scalar potential $\phi(\omega)$ are resonant scattered and plasma waves respectively coupled through intermediate nonresonant modes; other nonresonant idler modes outside this range are also generated. All of these need to be included to obtain accurate growth rates.

Figure 3 shows the growth for $q = 5$ in the directly back and forward scattered directions. The very narrow left most peak represents a hybrid of SRFS/RMI in which the two

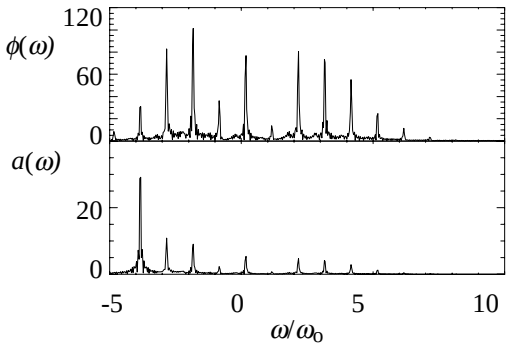

Fig. 2. Mode composition of a(ω), $\phi(\omega)$ versus frequency for lobe 4.1 when q=2.

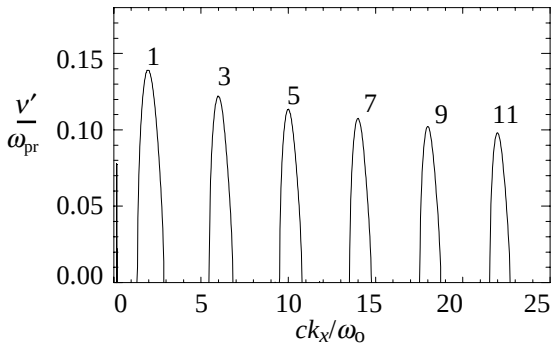

Fig. 3. Growth rate v'/ω_{pr} versus k_x when q=5 for exact back and forward scattering.

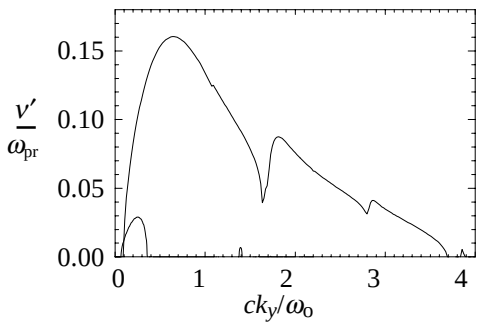

Fig. 4. RFI growth rate ν'/ω_{pr} versus k_y for q=0.5, 5.

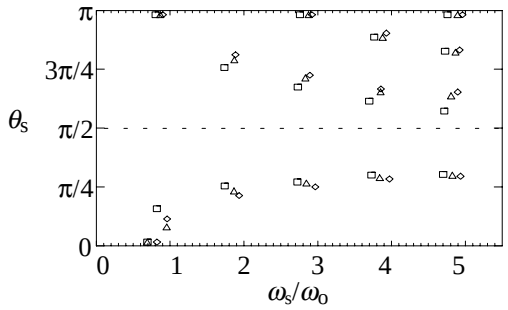

Fig. 5. Emission direction versus frequency when q =1(□),2(Δ),5(◊) for each lobe *n.m.*

instabilities overlap and interfere to produce a 6-mode instability consisting of Stokes and anti-Stokes em modes at $\omega_s \approx \omega_0 \pm \omega_{pr}$ and three electrostatic modes at $\omega \approx \omega_{pr}$ and $\omega \approx 2\omega_0 \pm \omega_{pr}$. The second peak (lobe 1.2) is the usual backscattering while the remaining peaks show backscattering at odd harmonics of the laser whose growth decays weakly with harmonic number n (when $q > 5$ this decay approximates the scaling of [1] where the growth reduces as $n^{-1/9}$ while at lower intensities the fall-off is much faster).

Figure 4 shows the growth rate for purely relativistic filamentation. This is a coupling of em modes through nonresonant purely growing transverse fluctuations. Successive peaks represent generation of exact laser harmonics; filamentation at the fundamental dominates where the transverse wavenumber locks at $k_y = 0.6\,\omega_{pr}/c$ for all $q > 1$.

Figure 5 indicates the emission angles versus frequency for radiation arising from each of the lobes in Figure 1. They show forward scattering $0 < \theta_s < \pi/2$ occurring predominantly into a single angle for each harmonic; this becomes more oblique with increasing harmonic number such that $\theta_s \to 54^o$. In backscattered directions, $\pi/2 < \theta_s < \pi$, emission occurs at $m_{\max}$ distinct angles for a given harmonic number n where $m_{\max} = (n+3)/2$ when n is odd, $m_{\max} = (n+2)/2$ for n even.

In conclusion, analysis carried out in the laser pulse proper frame provides a general, rugged and easily applied method for establishing the dispersion characteristics of electron parametric instabilities in which the pump may be anharmonic and the instability involve many modes.

References

[1] P. Sprangle and E. Esarey: Phys. Rev. Lett. **67**, 2021 (1991).
[2] A.S. Sakharov and V.I. Kirsanov: Plasma Phys. Rep. **21**, 596 (1995).
[3] J.M. Rax and N.J. Fisch: IEEE Trans. Plasma Sci. **21**, 105 (1993);
E. Esarey et al., **ibid**, 105.
[4] C.J. McKinstrie and R. Bingham: Phys. Fluids B **4**, 2626 (1992).
[5] B. Quesnel et al.: Phys. Rev. Lett. **78**, 2132 (1997);
S. Guérin et al.: Phys. Plasmas **2**, 2807 (1995).
[6] A.I. Akhiezar and R.V. Polovin: Sov. Phys. JETP **3**, 696 (1956).